

# Microarray Analysis Reveals Characteristic Changes of Host Cell Gene Expression in Response to Attenuated Modified Vaccinia Virus Ankara Infection of Human HeLa Cells

Susana Guerra,<sup>1</sup> Luis A. López-Fernández,<sup>2</sup> Raquel Conde,<sup>1</sup> Alberto Pascual-Montano,<sup>3</sup> Keith Harshman,<sup>2</sup> and Mariano Esteban<sup>1\*</sup>

*Department of Molecular and Cellular Biology,<sup>1</sup> Department of Immunology and Oncology,<sup>2</sup> and Biocomputing Unit,<sup>3</sup> Centro Nacional de Biotecnología, Consejo Superior de Investigaciones Científicas, Campus Universidad Autónoma, E-28049 Madrid, Spain*

Received 5 December 2003/Accepted 23 January 2004

**The potential use of the modified vaccinia virus Ankara (MVA) strain as a live recombinant vector to deliver antigens and elicit protective immune responses against infectious diseases demands a comprehensive understanding of the effect of MVA infection on human host gene expression. We used microarrays containing more than 15,000 human cDNAs to identify gene expression changes in human HeLa cell cultures at 2, 6, and 16 h postinfection. Clustering of the 410 differentially regulated genes identified 11 discrete gene clusters with altered expression patterns after MVA infection. Clusters 1 and 2 (accounting for 16.59% [68 of 410] of the genes) contained 68 transcripts showing a robust induction pattern that was maintained during the course of infection. Changes in cellular gene transcription detected by microarrays after MVA infection were confirmed for selected genes by Northern blot analysis and by real-time reverse transcription-PCR. Upregulated transcripts in clusters 1 and 2 included 20 genes implicated in immune responses, including interleukin 1A (IL-1A), IL-6, IL-7, IL-8, and IL-15 genes. MVA infection also stimulated the expression of NF- $\kappa$ B and components of the NF- $\kappa$ B signal transduction pathway, including p50 and TRAF-interacting protein. A marked increase in the expression of histone family members was also induced during MVA infection. Expression of the Wiskott-Aldrich syndrome family members WAS, WASF1, and the small GTP-binding protein RAC-1, which are involved in actin cytoskeleton reorganization, was enhanced after MVA infection. This study demonstrates that MVA infection triggered the induction of groups of genes, some of which may be involved in host resistance and immune modulation during virus infection.**

Interaction between mammalian cells and viruses has an impact on a diverse set of cellular processes. Many of these interactions are characterized by antiviral immune responses and changes in cellular transcriptional, translational, and trafficking machinery that in turn depend on the infection stage and the biological condition of the infected cell. The modified vaccinia virus (VV) Ankara (MVA), derived from the Ankara strain, is a highly attenuated virus. MVA has been passaged more than 500 times in chicken embryo fibroblasts. During the course of attenuation, 15% of the parental viral genome was lost (2, 25); the structural genes remained unaltered, but genes involved in immune evasion factors (4) and host range genes (1, 25, 42) have been deleted or fragmented. MVA produces an infectious cycle in chicken embryo fibroblasts and baby hamster kidney (BHK) cells but not in various human cell lines, including the HeLa cell line (7, 11). Although viral replication depends on cell type, blockade of the morphogenetic program in nonpermissive cells occurs in steps after the formation of immature viral forms, with no alteration in early or late viral gene expression (34, 36). In cultured cells, MVA recombinants produced levels of heterologous protein similar to or higher than those of VV-derived vectors (8, 33, 36). In

mammals, MVA recombinants induce protective immunity against a wide spectrum of pathogens (7, 18, 23, 24, 35, 37). MVA may be of use in the generation of live vaccines against infectious diseases and in cancer therapy due to its safety and its ability to evoke protection. The generation of such vaccines demands a comprehensive understanding of the effect of MVA infection on human host gene expression. With DNA microarray technology, the expression of several thousand individual genes can be monitored (19), and this technology has been used to identify cellular genes that are differentially expressed in response to infection with several animal viruses (5, 9, 16, 17, 20, 30, 41, 43). Here, we analyzed host gene expression changes in cultures of the human cervical carcinoma cell line HeLa at 2, 6, and 16 h postinfection by using cDNA microarray technology. During MVA infection, we found increased expression of cellular genes associated with the immune response and with a variety of cellular pathways. This study represents the first global analysis of the transcriptional response of HeLa cells to MVA infection.

## MATERIALS AND METHODS

**Cells, viruses, and infection conditions.** HeLa cells (from the American Type Culture Collection) were cultured in Dulbecco's medium supplemented with 10% newborn bovine serum and antibiotics. MVA was cultured in BHK-21 cells, purified by banding on sucrose gradients, and titrated on BHK-21 cells by immunostaining of fixed infected cultures with a polyclonal anti-VV protein antibody. The VV Western Reserve (WR) strain was grown in monkey BSC-40 cells, purified by sucrose gradient banding, and titrated on BSC-40 cells by

\* Corresponding author. Mailing address: Centro Nacional de Biotecnología, CSIC, Campus Universidad Autónoma, 28049 Madrid, Spain. Phone: (34) 91/585-4553. Fax: (34) 91/585-4506. E-mail: mesteban@cnb.uam.es.

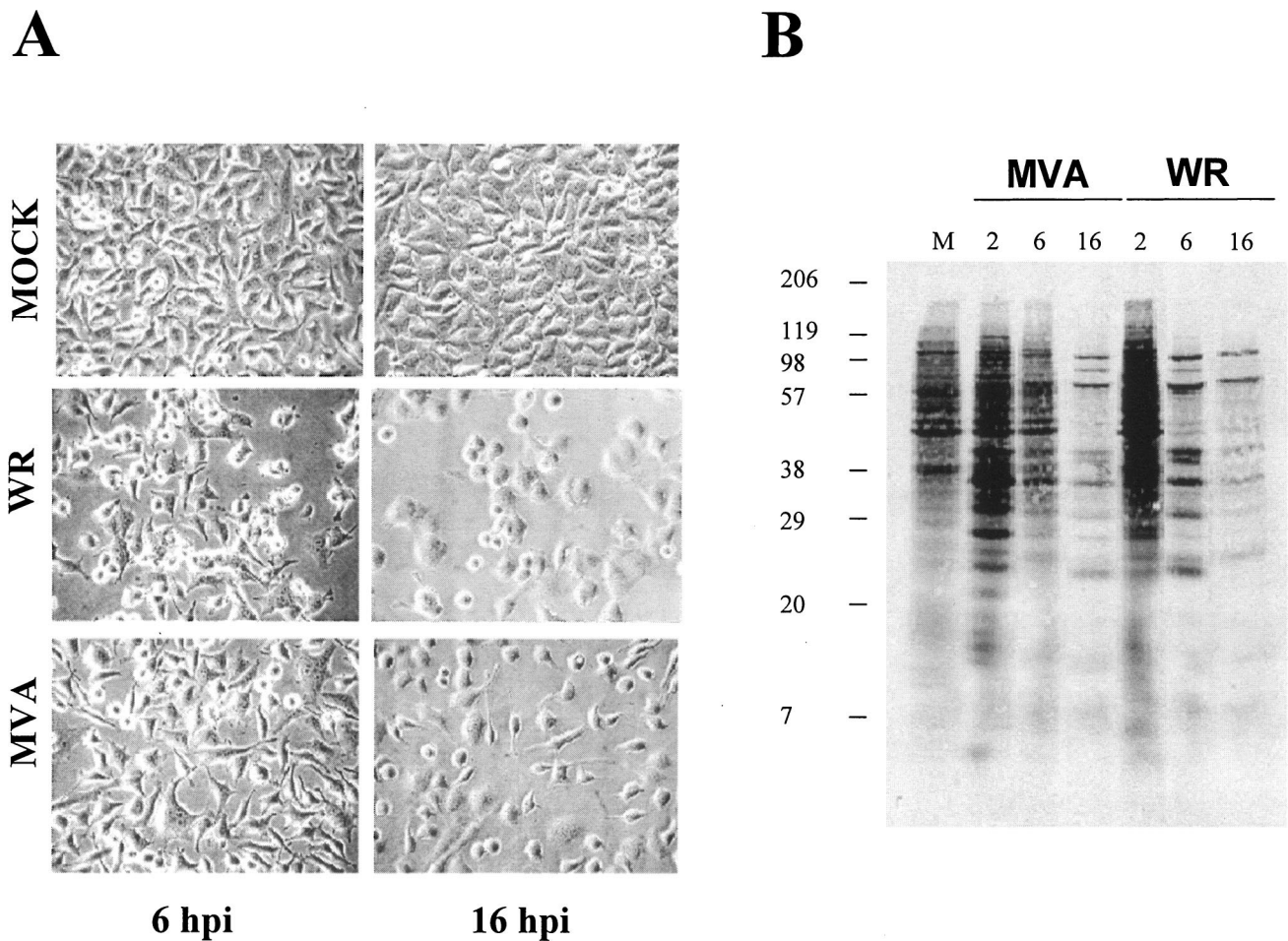


FIG. 1. Cytopathic effect and protein synthesis pattern of HeLa cells infected with VV WR and MVA strains. (A) Cell morphology after virus infection. Monolayer-cultured HeLa cells were infected with WR or MVA (5 PFU/cell), and CPEs were visualized by phase-contrast microscopy at the indicated times postinfection. hpi, hours postinfection. (B) Pattern of viral protein synthesis. HeLa cells were infected as described above and labeled with [<sup>35</sup>S]methionine (50  $\mu$ Ci, 30 min) at the times indicated. Cells lysates were analyzed by SDS-12% PAGE and visualized by autoradiography. Based on protein standards, molecular mass (in kDa) is indicated. Uninfected cells (M) served as the control. Postinfection times (in hours) are noted above the gels.

plaque assay. MVA and WR infections were carried out at a multiplicity of infection of 5 PFU/cell.

**Microarray fabrication.** The Research Genetics 40K sequence-verified clone human cDNA library (<http://www.resgen.com/products/SVHcDNA.php3>) was used to generate cDNA arrays as described previously (17). Slides contained 15,360 cDNAs, of which 13,295 correspond to known genes and 2,257 correspond to control genes. Printing on CMT-GAPS II slides (Corning) was performed with a Microgrid II (BioRobotics) at 22°C and 40 to 45% relative humidity.

**Microarray hybridization.** Total RNA was isolated from MVA-infected (5 PFU/cell) or mock-infected HeLa cells cultured in 10-cm plates with Ultra-spect-II RNA (Biotecx) by following the manufacturer's instructions. Uninfected samples were isolated at each infection time point and processed in parallel with infected cells. Two different samples of RNA from MVA-infected cells at 2, 6, and 16 h postinfection and RNA from corresponding mock-infected cells were processed for analysis. Each RNA was used in two different hybridizations. In one hybridization, the mock-infected sample was labeled with dUTP-Cy3 and the MVA-infected sample was labeled with dUTP-Cy5; in the other, the mock-infected sample was labeled with dUTP-Cy5 and the MVA-infected sample was labeled with dUTP-Cy3. Double labeling was used to abolish labeling and hybridization differences due to specific Cy-dUTP characteristics. A mixture containing 40  $\mu$ g of RNA, 150 pmol of oligo(dT)<sub>20</sub>, 0.5 mM dATP, 0.5 mM dGTP, 0.5 mM dCTP, 0.1 mM dTTP, 0.05 mM Cy3/Cy5 dUTP (Amersham), 1 $\times$  first-strand reaction buffer (Invitrogen), and 10 mM dithiothreitol in a volume of 38  $\mu$ l was heated (65°C, 5 min) and preincubated (42°C, 5 min), after which 400 U

of SuperScript II (Invitrogen) and 40 U of RNase Inhibitor (Roche) were added and the mixture was incubated (42°C, 2.5 h). The reaction was terminated with EDTA, and starting RNA template was removed by adding 2  $\mu$ l of 10 N NaOH, followed by incubation (20 min, 65°C). The reaction was neutralized by adding 4  $\mu$ l of 5 M acetic acid. Cy5 and Cy3 probes were mixed, and unincorporated dyes were removed by isopropanol precipitation. Probes were resuspended in deionized water; blocking reagents added to increase specificity were poly(A) (20  $\mu$ g; Sigma), tRNA (20  $\mu$ g; Sigma), and human Cot-1 DNA (20  $\mu$ g; Invitrogen). While probes were drying in a Speed-Vac, microarray slides were prehybridized in a mixture containing 6 $\times$  SSC (1 $\times$  SSC is 0.15 M NaCl plus 0.015 M sodium citrate), 0.5% sodium dodecyl sulfate (SDS), and 1% bovine serum albumin (42°C, 1 h), rinsed five times with water, and dried by centrifugation (563  $\times$  g, 1 min). Probes were resuspended in 40  $\mu$ l of hybridization buffer (50% formamide, 6 $\times$  SSC, 0.5% SDS, 5 $\times$  Denhardt's solution) and incubated with slides (42°C, 16 h) in hybridization chambers (Array-It) in a water bath in the dark. After incubation, slides were washed twice in 0.1 $\times$  SSC-0.1% SDS for 5 min each time and three times in 0.1 $\times$  SSC for 5 min each time. Finally, slides were dried by centrifugation as described above and scanned on a ScanArray 4000 (Packard Biosciences) by using ScanArray 3.1 software. Raw data were obtained from Cy5 and Cy3 images by using QuantArray 3.0 software (Packard Biosciences) and processed by using SOLAR software (BioALMA, Madrid, Spain). Briefly, background is subtracted from the signal,  $\log_{10}(\text{signal})$  is plotted versus  $\log_2(\text{ratio})$  and, a loess normalization is done to adjust most spots to  $\log_2(\text{ratio})$  0. This value is calculated for all four replicates and a table is obtained with mean signal,

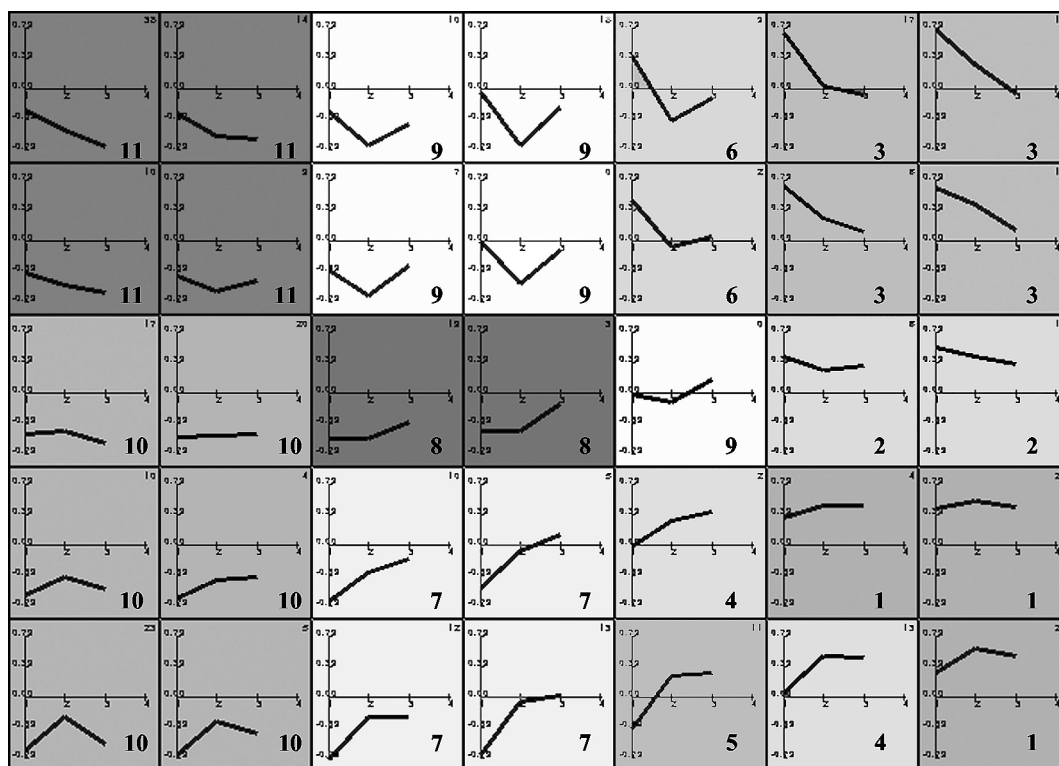


FIG. 2. Representation of 7-by-5 map obtained by the self-organizing maps algorithm, showing the gene expression cluster for MVA-infected HeLa cells. Each map node represents the average expression profile for a set of similar genes in the data set. Experimental points on the *x* axis are 1 for 2 h postinfection, 2 for 6 h postinfection, and 3 for 16 h postinfection. The *y* axis shows normalized expression values. Each cluster is shaded from white to gray and numbered from 1 to 11.

change (*n*-fold), log ratio, standard deviation of the log ratio, and *z* score (a measure of the proximity of one value [log ratio] to other values with similar signals) (32).

**Gene expression analysis.** The original data set containing 13,295 clones per slide was prepared for clustering. Genes with an interreplicate standard deviation of  $>1$  were removed from the analysis. The resulting data set was reduced to 9,749 transcripts that showed a consistent expression value among the four replicates. The *z* score value was used to eliminate genes that did not show significant expression under at least one experimental condition (32). In this way, only genes with *z* scores of  $>2$  were selected for clustering. A new data set was created with the 410 transcripts that successfully passed through the filter. After the data were preprocessed, genes were clustered by using Kohonen's classical self-organizing map (12, 22, 40). The resulting 7-by-5 map was analyzed by using the Engene software package (15), available at <http://www.engene.cnb.uam.es>.

**Quantitative real-time RT-PCR.** RNA (1  $\mu$ g) was reverse transcribed by using the Superscript first-strand synthesis system for reverse transcription-PCR (RT-PCR) (Invitrogen). A 1:40 dilution of the RT reaction mixture was used for quantitative PCR. Primers and the probe set used to amplify H2BFB, PCNT2, WASF1, WAS, interleukin 7 (IL-7), IL-6, IFNG, APEXL2, and FLJ20643 were purchased from Applied Biosystems. RT-PCRs were performed by using Assay-on-Demand optimized to work with TaqMan Universal PCR Master Mix, No AmpErase UNG, as previously described (17). All samples were assayed in duplicate. Threshold cycle values were used to plot a standard curve in which the threshold cycle value decreased in linear proportion to the log of the template copy number. The correlation values of standard curves were always  $>99\%$ .

**Western blot.** HeLa cells were infected at 5 PFU/cell with MVA or WR and collected at 2, 6, and 16 h postinfection in lysis buffer (50 mM Tris-HCl [pH 8.0], 0.5 M NaCl, 10% NP-40, 1% SDS). Equal amounts of protein lysates (10  $\mu$ g) were separated by SDS-polyacrylamide gel electrophoresis (SDS-PAGE) on 14 or 8% gels, transferred to nitrocellulose membranes, and incubated with primary antiactin (Sigma), antitubulin (Sigma), anti-NF- $\kappa$ B (Santa Cruz), anti-RAC-1 (kindly provided by J. C. Gallego), anti-WAS (Santa Cruz), and anti-WAVE (Santa Cruz), followed by peroxidase-conjugated mouse and rabbit secondary antibodies. The blots were developed by using the ECL protocol (Amersham).

**Analysis of [ $^{35}$ S]methionine labeled proteins.** HeLa cell monolayers in 12-well plates were mock infected or infected with WR or MVA at 5 PFU/cell. At the indicated times post infection, cells were washed with methionine-free medium and incubated with methionine-free medium containing 50  $\mu$ Ci of [ $^{35}$ S]methionine per well (30 min, 37°C). Proteins in cell extracts prepared in lysis buffer were fractionated by SDS-12% PAGE and developed by autoradiography.

**ELISA.** Secreted IL-6 and gamma interferon (IFN- $\gamma$ ) in the medium of MVA- or WR-infected HeLa cells were measured with the quantitative human IL-6 and IFN- $\gamma$  kit (BD Biosciences). Aliquots (100  $\mu$ l) of supernatant from uninfected or infected HeLa cells at 2, 6, and 16 h postinfection were used for ELISA according to the manufacturer's instructions. Captured IL-6 and IFN- $\gamma$  were quantified at 450 nm with a spectrophotometer. Duplicate samples were measured in two independent experiments.

## RESULTS

**Gene expression analysis.** To study the cellular transcriptional response after MVA infection, we first defined the cytopathic effect (CPE) and shutoff of MVA-infected HeLa cells compared to cells infected with the WR strain. WR produced a pronounced CPE at 6 and 16 h postinfection, and this CPE was reduced in MVA-infected cells (Fig. 1A). At a multiplicity of infection of 5 PFU/cell, over 99% of the cells were infected. At 16 h postinfection, more rounded cells were observed after WR infection, whereas MVA produced rounded and bipolar cells, as previously noted (14). The pattern of protein synthesis is shown in Fig. 1B. At 6 h postinfection, WR-infected cells showed a more evident shutoff than MVA-infected cells, while at 16 h postinfection, shutoffs induced by both viruses were similar.

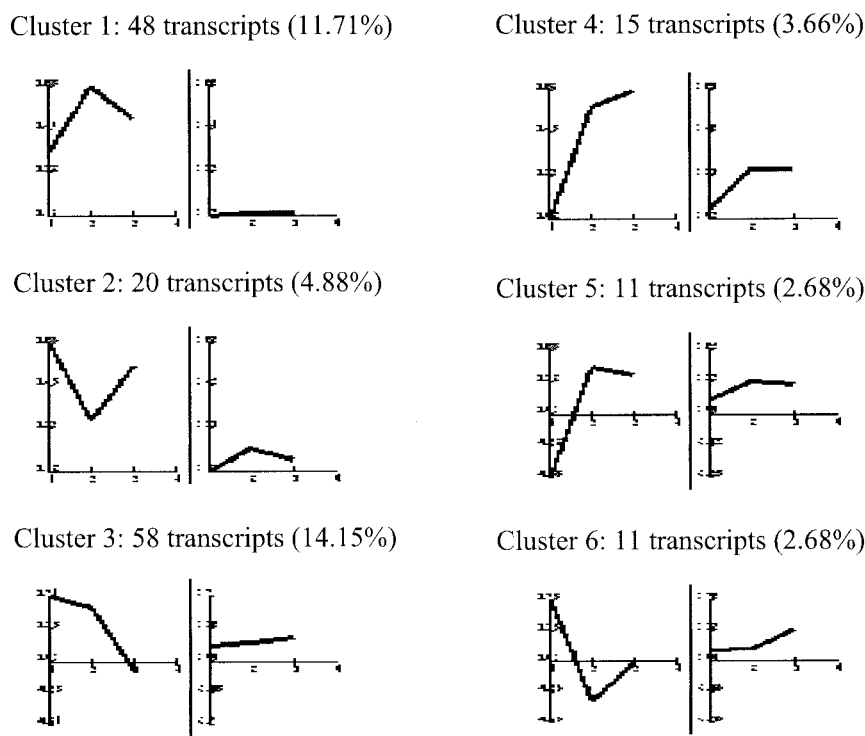


FIG. 3. Characteristic expression patterns represented in clusters 1 to 6. Shown are mean values (left) and standard deviations (right) of the expression profiles of genes assigned to each cluster. Experimental points on the  $x$  axis are 1 for 2 h postinfection, 2 for 6 h postinfection, and 3 for 16 h postinfection. The  $y$  axis shows normalized expression values. The values in parentheses are percentages of genes in each cluster with reference to the total of 410 differentially expressed genes.

We performed cDNA microarray analysis to determine the relative abundance of specific mRNAs induced in MVA-infected cells compared to that induced in mock-infected cells. The gene expression clusters of the 410 differentially regulated genes are depicted in Fig. 2. Detailed profile analysis led us to group the genes into 11 main clusters according to their behavior at the three time points of MVA infection by using Engene software (15). Clusters 1 and 2 contained 68 transcripts, representing 16.59% of the 410 genes, showing a robust induction pattern that was maintained during the course of infection. Cluster 3 contained 58 transcripts (14.15%), including genes with a generalized induction pattern maintained from 2 to 6 h postinfection that returned to basal levels at 16 h postinfection. Cluster 4 had 15 transcripts (3.66%), with an upregulation pattern maintained from 6 to 16 h postinfection. Cluster 5 contained 11 transcripts (2.68%) that were downregulated at 2 h postinfection and upregulated at 6 and 16 h postinfection. Cluster 6 contained 11 transcripts (2.68%) with upregulated expression only at 2 h postinfection. The average profiles for clusters 1 to 6 are shown in Fig. 3; these six clusters include genes involved in adhesion, cell cycles, immune response, signal transmission, metabolic pathways, and other vital cell processes. Representative human genes upregulated by MVA infection in clusters 1 to 6 are shown in Table 1. Genes whose expression was repressed after MVA infection represented 60.24% of the 410 genes; representative human genes downregulated by MVA in clusters 7 to 11 are detailed in Table 2.

**Confirmation of microarray data for selected genes by Northern blot analysis and real-time RT-PCR.** Selected genes with distinct expression patterns after MVA infection, as identified by microarray analysis, were chosen for target verification by Northern blotting. Total RNA was purified from uninfected or MVA-infected cells at 2, 6, and 16 h postinfection, fractionated by gel electrophoresis, blotted, and probed by using  $^{32}\text{P}$ -labeled PCR products that were spotted on the microarray. The RNA preparation used for this analysis was the same as that used in the microarray. The amount of RNA on the blot was normalized based on rRNA content. The Northern blot analysis confirmed microarray results in all cases (Fig. 4). Whereas the expression pattern of histone family member N (H2AFN) was weakly detected in mock-infected cells, strong activation compared to that for the uninfected control was observed at 2, 6, and 16 h postinfection. A similar expression pattern was observed for WAS protein family member 1 (WASF1). Peaks of histone F gene H2FB mRNA expression were reached at 2 and 6 h postinfection. A constitutive expression pattern of the apurinic/apyrimidinic endonuclease gene (APEXL2) and the EST FLJ20643 was observed in the presence and in the absence of MVA.

As an alternative to the Northern blot analysis, real-time RT-PCR was used to verify the transcriptional changes in selected genes detected by microarray analysis. Six upregulated genes (H2BFB, PCNT2, WASF1, WAS, IL-7, and IL-6) and three unaltered genes (IFNG, APEXL2, and FLJ20643) were analyzed; hypoxanthine phosphoribosyltransferase was used as

TABLE 1. Representative human genes in clusters 1 to 6 (upregulated by MVA)<sup>a</sup>

Function or protein description and gene name	Accession no.	Gene symbol	Change (fold) at time (h) postinfection		
			2.00	6.00	16.00
<b>Cluster 1</b>					
Adhesion molecules and cytoskeleton					
Connective tissue growth factor	AA598794	CTGF	5.78	4.5	2.17
Pericentrin	N45326	PCNT	3.94	3.14	2.38
Fibroblast growth factor 9 (glia-activating factor)	AA946776	FGF9	2.05	2.58	1.41
Attractin	AA683500	ATRNL1	2.16	2.6	1.41
Adaptin, alpha A	AI018208	ADTAA	2.95	1.56	1.78
Calmeglin	AA778675	CLGN	2.01	2.43	1.29
filamin A, alpha (actin-binding protein-280)	AA478436	FLNA	3.07	3.63	2.79
Collagen, type VII, alpha 1 (epidermolysis bullosa, dystrophic, dominant, and recessive)	AA598507	COL7A1	2.35	2.71	1.47
Cell cycle, DNA damage, apoptosis					
Immediate early protein	AA496359	ETR101	3.12	2.81	2.11
CDC7 (cell division cycle 7, <i>Saccharomyces cerevisiae</i> , homolog)-like 1	N62245	CDC7L1	2.17	2.36	1.72
Jun B proto-oncogene	N94468	JUNB	2.93	3.92	1.06
Histones					
H3 histone family, member B	AI399887	H3FB	16.34	15.67	21.71
H4 histone family, member D	AI653010	H4FD	12.38	24.93	24.93
H2B histone family, member B	AA885642	H2BFB	9.92	10.20	17.03
H2A histone family, member N	AI095013	H2AFN	7.46	4.82	11.55
Immune response					
Interleukin 7	AI539460	IL7	6.1	5.3	3.2
Interleukin 15	N59270	IL15	2.91	2.68	1.59
Interleukin 8	AA102526	IL8	2.55	2.22	1.84
Interleukin 6 (interferon, beta 2)	N98591	IL6	2.65	2.14	1.56
CD47 antigen (Rh-related antigen, integrin-associated signal transducer)	AA455448	CD47	5.35	4.08	3.16
CD80 antigen (CD28 antigen ligand 1, B7-1 antigen)	AA983817	CD80	4.29	3.36	2.57
Interleukin 1, alpha	AA936768	IL1A	2.36	2.31	2.44
Tumor necrosis factor, alpha-induced protein 3	AA476272	TNFAIP3	2.65	2.23	1.96
CD8 antigen, beta polypeptide 1 (p37)	AA293671	CD8B1	2.1	2.53	2.47
TNF receptor-associated factor 3	AA504259	TRAF3	2.6	2.30	1.67
Interleukin 22 receptor	AA132964	IL22R	3.32	3.94	2.2
Tumor necrosis factor receptor superfamily, member 17	AA987627	TNFRSF17	2.97	2.58	2.24
Miscellaneous					
Surfactant, pulmonary-associated protein D	AI289238	SFTPD	2.73	4.38	4.14
Thymosin beta 4 X chromosome	AA634103	TMSB4X	3.81	5.7	2.91
Human erythroid isoform protein 4.1 mRNA, complete cds	AA703141		2.87	3.23	1.93
Signal transmission					
Dopachrome tautomerase (dopachrome delta-isomerase, tyrosine-related protein 2)	AA478553	DCT	3.76	19.16	1.79
Nuclear factor of kappa light polypeptide gene enhancer in B-cells 2 (p49/p100)	AA952897	NFKB2	2.03	2.22	2.34
Mitogen-activated protein kinase kinase 5	AA250966	MAP2K5	2.37	2.74	1.69
Nuclear factor (erythroid-derived 2)-like 3	W76339	NFE2L3	2.36	2.36	2.52
Adenosine A2a receptor	N57553	ADORA2A	3.89	4.14	4.11
Ras-related C3 botulinum toxin substrate 1 (Rho family, small GTP-binding protein RAC-1)	AA626787	RAC1	2.5	1.85	2.9
Pronapsin A	AI369218	NAP1	2.28	3.63	2.43
Transcription, replication, translation, degradation machinery, protein modification					
TATA box binding protein-associated factor, RNA polymerase II, F, 55 kDa	AA461518	TAF2F	2.87	2.75	2.82
Transcriptional repressor	H89996	CTCF	2.55	2.2	2.23
Protein phosphatase 2 (formerly 2A), regulatory subunit B (PR 52), alpha isoform	AA598795	PPP2R2A	2.49	2.02	1.68
WASP family					
Wiskott-Aldrich syndrome (eczema-thrombocytopenia)	H61193	WAS	2.58	2.25	2.61
WAS protein family, member 1	N59851	WASF1	3.01	2.66	2.11
Vasoactive intestinal peptide	AI217172	VIP	2.01	2.58	2.32
<b>Cluster 2</b>					
Adhesion molecules and cytoskeleton					
Inter-alpha (globulin) inhibitor H4 (plasma Kallikrein-sensitive glycoprotein)	N73625	ITIH4	2.99	2.43	1.16

Continued on facing page

TABLE 1—Continued

Function or protein description and gene name	Accession no.	Gene symbol	Change (fold) at time (h) postinfection		
			2.00	6.00	16.00
Flamin C, gamma (actin-binding protein-280)	AI675658	FLNC	2.95	2.44	1.15
Elastase 1, pancreatic	AA845015	ELA1	2.9	1.59	1.25
Claudin 3	AA039323	CLDN3	2.54	2.48	1.32
Cadherin 15, M-cadherin (myotubule)	AI571806	CDH15	2.95	2.46	1.15
Cell cycle, DNA damage, apoptosis					
Cell division cycle 25A	H59260	CDC25A	2.02	1.35	2.14
RAB6, member of RAS oncogene family	AA934745	RAB6	2.97	1.34	1.64
DEAD/H (Asp-Glu-Ala-Asp/His) box polypeptide 11 ( <i>Saccharomyces cerevisiae</i> CHL1-like helicase)	AA402879	DDX11	2.91	1.48	1.37
Miscellaneous					
Solute carrier family 28 (sodium-coupled nucleoside transporter), member 1	AI344386	SLC28A1	2.93	1.66	1.74
Dual-specificity phosphatase 2	AA759046	DUSP2	3.92	3.58	1.00
Immune response					
Nuclear factor of activated T cells, cytoplasmic 3	AA179812	NFATC3	3.46	2.97	1.30
Tumor necrosis factor receptor superfamily, member 14 (herpesvirus entry mediator)	AI245559	TNFRSF14	2.84	2.28	1.68
Tumor necrosis factor (ligand) superfamily, member 7	AI347622	TNFSF7	2.99	1.64	1.3
Interferon-stimulated protein, 15 kDa	AA406020	ISG15	3.12	2.93	1.61
Karyopherin (importin) beta 1	AA251527	KPNB1	2.49	2.1	1.26
Cluster 3					
Adhesion molecules and cytoskeleton					
Prefoldin 4	AA253430	PFDN4	2.08	1.49	1.17
Coronin, actin-binding protein, 2A	AA983765	CORO2A	2.04	1.73	1.04
Kinesin family member 5A	AA984728	KIF5A	2.05	1.88	1.73
Integrin beta 3 (alternatively spliced, clone beta 3C)	AA037229	ITGB3	2.12	1.72	1.41
Cell cycle, DNA damage, apoptosis					
RAB2, member RAS oncogene family-like	AA401972	RAB2L	2.33	1.78	1.38
V-myc avian myelocytomatosis viral oncogene homolog	AA464600	MYC	2.22	1.53	1.05
V-jun avian sarcoma virus 17 oncogene homolog	W96155	JUN	2.17	2.02	1.31
Immune response					
CD1A antigen, a polypeptide	AI240210	CD1A	2.2	1.39	1.45
CD28 antigen (Tp44)	AI375736	CD28	2.16	1.49	1.27
Interferon, alpha-inducible protein 27	AA157813	IFI27	2.15	1.37	1.92
Transporters					
Solute carrier family 25 (mitochondrial carrier; Graves disease autoantigen) member 16	AA411554	SLC25A16	2.11	1.71	1.57
Solute carrier family 6 (neurotransmitter transporter, taurine), member 6	AI688443	SLC6A6	2.3	1.65	1.43
Signal transmission					
Regulator of nonsense transcripts 1	AA156342	RENT1	2.48	2.38	1.56
Nuclear factor of kappa light polypeptide gene enhancer in B-cells inhibitor, epsilon	AA953975	NFKBIE	2.41	1.61	1.12
Zinc finger protein 173	AA490855	ZNF173	2.31	2.14	1.39
Cluster 4					
Histones					
H4 histone family, member G	AA868008	H4FG	1.91	2.58	3.34
Immune response					
B7 protein	N90281	B7	1.97	1.75	3.53
Metabolism					
Protein disulfide isomerase related protein (calcium-binding protein, intestine related)	N59626	ERP70	1.34	2.87	2.06
Miscellaneous					
Human putative tumor suppressor (LUCA15) mRNA, complete cds	AA456007		1.52	2.55	2.28
RAE1 (RNA export 1, <i>Schizosaccharomyces pombe</i> ) homolog	AA504128	RAE1	1.91	2.04	1.95
Cluster 5					
Adhesion molecules and cytoskeleton					
Dynein, cytoplasmic, light intermediate polypeptide 2	AA490963	DNCLI2	0.71	2.47	1.82
Cluster 6					
Adhesion molecules and cytoskeleton					
Lamin B1	AA983462	LMNB1	2.00	1.54	1.91

<sup>a</sup> Genes in each cluster are grouped according to predicted biological function.

TABLE 2. Representative human genes in clusters 7 to 11 (downregulated by MVA)<sup>a</sup>

Function or protein description and gene name	Accession no.	Gene symbol	Change (fold) at time (h) postinfection		
			2.00	6.00	16.00
Cluster 7					
Enzymes					
3-Oxoacid coenzymeA transferase	R40897	OXCT	0.60	0.67	1.05
Aldehyde dehydrogenase 7	N93686	ALDH7	0.68	0.66	1.02
Acetylcholinesterase (YT blood group)	R85241	ACHE	0.71	0.67	1.10
Transcription					
Adenosine A3 receptor	AA863086	ADORA3	0.97	0.79	1.73
Adenosine deaminase	AA683578	ADA	0.84	0.58	1.49
Cluster 8					
ATP synthase					
ATP synthase, H <sup>+</sup> transporting, mitochondrial F <sub>0</sub> complex, subunit c (subunit 9), isoform 2	AA455126	ATP5G2	0.53	0.40	1.12
Translation					
Eukaryotic translation elongation factor 1 alpha 2	AI368766	EEF1A2	0.93	0.66	0.91
Eukaryotic translation initiation factor 4 gamma 1	R37276	EIF4G1	0.93	0.69	0.90
Polymerase (DNA directed), beta	R44427	POLB	0.88	0.73	0.64
Cluster 9					
Cell cycle, DNA damage, apoptosis					
v-maf musculoaponeurotic fibrosarcoma (avian) oncogene family, protein G	AA045436	MAFG	0.85	0.5	0.66
BCL2-associated athanogene	AI017240	BAG1	0.86	0.84	0.68
Cyclin-dependent kinase inhibitor 2C (p18, inhibits CDK4)	N72115	CDKN2C	0.82	0.81	0.68
Cytochrome					
Cytochrome P450, subfamily I (aromatic compound-inducible), polypeptide 1	AA418907	CYP1A1	0.86	0.87	0.68
Cytochrome P450, subfamily I (dioxin-inducible), polypeptide 1 (glaucoma 3, primary infantile)	AA448157	CYP1B1	0.84	0.80	0.66
Cytoskeleton					
Actin-related protein 2/3 complex, subunit 5 (16 kDa)	W55964	ARPC5	0.82	0.82	0.6
Actinin, alpha 1	AA669042	ACTN1	0.97	0.67	0.75
Actinin, alpha 3	AA196000	ACTN3	0.83	0.76	0.51
Annexin A1	H63077	ANXA1	0.97	0.7	0.67
Collagen, type III, alpha 1 (Ehlers-Danlos syndrome type IV, autosomal dominant)	T98612	COL3A1	0.85	0.41	1.25
Collagen, type IX, alpha 1	N69335	COL9A1	0.84	0.65	0.66
Collagen, type V, alpha 2	AA461456	COL5A2	0.84	0.67	0.51
Dextrin (actin depolymerizing factor)	AA424824	ADF	0.84	0.55	0.43
Keratin 7	AA485959	KRT7	0.83	0.63	0.53
Moesin	R22977	MSN	0.85	0.55	0.44
Myosin, light polypeptide 4, alkali; atrial, embryonic	AA705225	MYL4	0.87	0.81	0.35
Myosin, light polypeptide 6, alkali, smooth muscle and nonmuscle	AA488346	MYL6	0.85	0.58	0.45
Prefoldin 5	AA446453	PFDN5	0.85	0.62	0.58
Tubulin, gamma polypeptide	T77733	TUBG1	0.87	0.40	0.69
Enzymes					
Acetylserotonin N-methyltransferase-like	AA427398	ASMTL	0.84	0.84	0.67
Casein kinase 1, alpha 1	AA625758	SSP29	0.98	0.72	0.58
NADH dehydrogenase (ubiquinone) 1 beta subcomplex, 3 (12 kDa, B12)	AI675527	NDUFB3	0.86	0.6	0.62
NADH dehydrogenase (ubiquinone) 1, subcomplex unknown, 1 (6 kDa, KFYI)	AA460251	NDUFC1	0.81	0.58	0.54
NADH dehydrogenase (ubiquinone) 1, subcomplex unknown, 1 (6 kDa, KFYI)	AA460251	NDUFC1	0.81	0.58	0.54
NADH dehydrogenase (ubiquinone) 1 beta subcomplex, 7 (18 kDa, B18)	AA428058	NDUFB7	0.86	0.43	0.46
Ribosomal proteins					
Ribosomal protein L22	AI688090	RPL22	0.96	0.72	0.56
Ribosomal protein L35	AA625634	RPL35	0.93	0.66	0.76
Ribosomal protein S10	AI611010	RPS10	0.96	0.72	0.65
Ribosomal protein S12	AI689992	RPS12	0.97	0.69	0.62
Ribosomal protein S23	N73091	RPS23	0.94	0.66	0.71
Ribosomal protein S27a	AA625632	RPS27A	0.85	0.58	0.72
Ribosomal protein S28	AA856556	RPS28	0.89	0.63	0.69
Ribosomal protein S5	AA456616	RPS5	0.95	0.71	0.65

Continued on facing page

TABLE 2—Continued

Function or protein description and gene name	Accession no.	Gene symbol	Change (fold) at time (h) postinfection		
			2.00	6.00	16.00
Degradation machinery					
Proteasome (prosome, macropain) 26S subunit, ATPase 3	AA987573	PSMC3	0.98	0.67	0.69
Proteasome (prosome, macropain) activator subunit 2 (PA28 beta)	H65395	PSME2	0.98	0.60	0.59
Proteasome (prosome, macropain) subunit, beta type 1	T68758	PSMB1	0.98	0.69	0.73
Proteasome (prosome, macropain) subunit, beta type 3	AA620580	PSMB3	0.98	0.69	0.71
Ubiquinol-cytochrome <i>c</i> reductase binding protein	AA664284	UQCRB	0.81	0.64	0.56
Ubiquitin-specific protease 4 (proto-oncogene)	AA454143	USP4	0.81	0.62	0.54
Transcription					
Transcription factor CP2	AA488618	TFCP2	0.81	0.58	0.49
Adenine nucleotide translocator 3 (liver)	AA663439	SLC25A6	0.98	0.58	0.44
Transcription elongation factor B (SIII), polypeptide 3 (110 kDa, elongin A)	AA133129	TCEB3	0.82	0.69	0.70
General transcription factor IIIH, polypeptide 3 (34 kDa subunit)	AA460838	GTF2H3	0.96	0.68	0.74
Polymerase (RNA) II (DNA directed) polypeptide G	AA477428	POLR2G	0.92	0.75	0.60
Polymerase (RNA) II (DNA directed) polypeptide I (14.5 kDa)	AA777192	POLR2I	0.82	0.58	0.42
Translation					
Eukaryotic translation initiation factor 3, subunit 6 (48 kDa)	AA669674	EIF3S6	0.95	0.70	0.55
Eukaryotic translation initiation factor 3, subunit 2 (beta, 36 kDa)	AA936783	EIF3S2	0.91	0.52	0.42
Cluster 10					
Cytoskeleton					
Tubulin, beta 2	A1000256	TUBB2	0.84	0.79	0.48
Collagen, type V, alpha 1	R75635	COL5A1	0.56	0.96	0.67
Enzymes					
Aldose reductase-like 1	A1301329	ALDRLn	0.63	0.84	0.79
Carboxypeptidase B2 (plasma)	H47838	CPB2	0.64	0.68	0.88
Carnitine palmitoyltransferase II	A1369287	CPT2	0.60	0.72	0.63
Acyl-coenzyme A dehydrogenase, very long chain	AA464163	ACADVL	0.70	0.64	0.74
1-Acylglycerol-3-phosphate <i>O</i> -acyltransferase 1 (lysophosphatidic acid acyltransferase, alpha)	AA458922	AGPAT1	0.62	0.65	0.72
Casein kinase 2, beta polypeptide	AA994790	CSNK2B	0.65	0.43	0.50
COX11 (yeast) homolog, cytochrome <i>c</i> oxidase assembly protein	AA457644	COX11	0.71	0.74	0.84
Creatine kinase, mitochondrial 1 (ubiquitous)	A1369378	CKMT1	0.69	0.76	0.64
Cystathionine-beta-synthase	AA430367	CBS	0.68	0.90	0.71
Dolichyl-phosphate mannosyltransferase polypeptide 1, catalytic subunit	AA004759	DPM1	0.66	0.76	0.68
Ephrin-A1	AA857015	EFNA1	0.57	0.74	0.69
NADH dehydrogenase (ubiquinone) Fe-S protein 8 (23 kDa) (NADH-coenzyme Q reductase)	AA127014	NDUFSS	0.63	0.55	0.55
7-Dehydrocholesterol reductase	A1652764	DHCR7	0.72	0.63	0.64
Immune response					
Erythrocyte membrane protein band 4.1-like 1	R71689	EPB41L1	0.84	0.41	0.45
Interferon gamma receptor 1	H11482	IFNGR1	0.70	0.41	0.44
Macrophage stimulating 1 (hepatocyte growth factor-like)	T47813	MST1	0.68	0.65	0.74
Splicing					
Splicing factor proline/glutamine rich (polypyrimidine tract-binding protein-associated)	AA418910	SFPQ	0.74	1.12	0.66
Splicing factor, arginine/serine-rich 11	H56944	SFRS11	0.64	0.129	0.30
Degradation machinery					
Ubiquinol-cytochrome <i>c</i> reductase core protein II	AA663058	UQCRC2	0.73	0.51	0.70
Ubiquitin-conjugating enzyme E2L 3	AA487058	UBE2L3	0.65	0.46	0.62
Ubiquitin-specific protease 15	AA253442	USP15	0.84	0.59	0.64
Transcription					
General transcription factor IIIC, polypeptide 1 (alpha subunit, 220 kDa)	AA843718	GTF3C1	0.70	0.81	0.86
Polymerase (RNA) II (DNA directed) polypeptide K (7.0 kDa)	AA458646	POLR2K	0.66	0.65	0.71
Ribophorin II	AA991856	RPN2	0.52	0.60	0.54
B-cell CLL/lymphoma 10	AA456036	BCL10	0.70	0.88	0.67
Adenine nucleotide translocator 3 (liver)	AA496376	SLC25A6	0.69	0.59	0.54

Continued on following page

TABLE 2—Continued

Function or protein description and gene name	Accession no.	Gene symbol	Change (fold) at time (h) postinfection		
			2.00	6.00	16.00
Translation					
Human translation initiation factor eIF-2alpha mRNA, 3' untranslated region	AA424956		0.69	0.72	0.65
Eukaryotic translation initiation factor 3, subunit 9 (eta, 116 kDa)	AA676471	EIF3S9	0.70	0.53	0.70
Cluster 11					
ATP synthase					
ATP synthase, H <sup>+</sup> transporting, mitochondrial F <sub>0</sub> complex, subunit f, isoform 2	AA453995	ATP5J2	0.46	0.25	0.25
ATP synthase, H <sup>+</sup> transporting, mitochondrial F <sub>1</sub> complex, beta polypeptide	AA708298	ATP5B	0.42	0.17	0.16
ATP synthase, H <sup>+</sup> transporting, mitochondrial F <sub>1</sub> complex, O subunit	AA873577	ATP5O	0.66	0.38	0.19
ATP synthase, H <sup>+</sup> transporting, mitochondrial F <sub>0</sub> complex, subunit f, isoform 2	AA453995	ATP5J2	0.52	0.61	0.25
ATP synthase, H <sup>+</sup> transporting, mitochondrial F <sub>1</sub> F <sub>0</sub> , subunit g	AA126313	ATP5JG	0.46	0.25	0.36
ATP synthase, H <sup>+</sup> transporting, mitochondrial F <sub>0</sub> complex, subunit c (subunit 9) Isoform 3	H47080	ATP5G3	0.25	0.31	0.36
ATP synthase, H <sup>+</sup> transporting, mitochondrial F <sub>1</sub> complex, O subunit	AA873577	ATP5O	0.36	0.53	0.23
ATP synthase, H <sup>+</sup> transporting, mitochondrial F <sub>0</sub> complex, subunit e	AA431433	ATP5I	0.44	0.39	0.10
Cell cycle, DNA damage, apoptosis					
DEAD/H (Asp-Glu-Ala-Asp/His) box polypeptide 8 (RNA helicase)	AI190747	DDX8	0.67	0.65	0.45
DEAD/H (Asp-Glu-Ala-Asp/His) box polypeptide 9	AA458801	DDX9	0.78	0.79	0.55
B-cell CLL/lymphoma 7A	H90147	BCL7A	0.74	0.5	0.52
BCL2-antagonist of cell death	AA460291	BAD	0.67	0.65	0.45
Caspase 3, apoptosis-related cysteine protease	AA011446	CASP3	0.67	0.57	0.54
CDC37 (cell division cycle 37, <i>Saccharomyces cerevisiae</i> , homolog)	AA458870	CDC37	0.67	0.45	0.54
Cell division cycle 34	H20743	CDC34	0.65	0.56	0.51
Cell division cycle 42 (GTP-binding protein, 25 kDa)	AA630164	CDC42	0.67	0.4	0.42
Colony-stimulating factor 1 receptor	T46880	CSF1R	0.67	0.45	0.54
Cyclin-dependent kinase inhibitor 1C (p57, Kip2)	AI676118	CDKN1C	0.67	0.57	0.54
Neuroblastoma candidate region, suppression of tumorigenicity 1	AA598830	NBL1	0.79	0.53	0.72
Cytochrome					
Cytochrome <i>c</i> oxidase subunit Vb	AI688757	COX5B	0.64	0.38	0.33
Cytochrome <i>c</i> oxidase subunit VIa polypeptide 1	AA482243	COX6A1	0.86	0.42	0.37
Cytochrome <i>c</i> oxidase subunit VIIa polypeptide 1 (muscle)	AA872125	COX7A1	0.73	0.53	0.58
Cytochrome <i>c</i> oxidase subunit VIIa polypeptide 2 (liver)	AI002403	COX7A2	0.9	0.75	0.67
Cytochrome <i>c</i> oxidase subunit VIIC	AA629719	COX7C	0.3	0.53	0.52
Cytochrome <i>c</i> -1	AA447774	CYC1	0.71	0.37	0.23
Cytoskeleton					
Acid phosphatase 2, lysosomal	T48864	ACP2	0.77	0.65	0.4
Actin, alpha 2, smooth muscle, aorta	AA634006	ACTA2	0.76	0.47	0.44
Actin, gamma 2, smooth muscle, enteric	T60048	ACTG2	0.65	0.47	0.42
Collagen, type IV, alpha 2	AA430540	COL4A2	0.74	0.26	0.34
Collagen, type IV, alpha 5 (Alport syndrome)	AA953254	COL4A5	0.84	0.35	0.18
Collagen, type VI, alpha 2	AA633747	COL6A2	0.74	0.51	0.59
Keratin 16 (focal nonepidermolytic palmoplantar keratoderma)	AA928454	KRT16	0.26	0.2	0.16
Myosin, heavy polypeptide 9, nonmuscle	T69926	MYH9	0.48	0.65	0.25
Myosin, light polypeptide 1, alkali; skeletal, fast	T52894	MYL1	0.78	0.6	0.53
Keratin 19	AA464250	KRT19	0.25	0.32	0.2
Profilin 2	AA040703	PFN2	0.76	0.65	0.45
Rho GDP dissociation inhibitor alpha	AA459400	ARHGDI A	0.35	0.24	0.39
Tubulin-specific chaperone d	AI668870	TBCD	0.85	0.57	0.49
Tubulin, alpha 2	AA626698	TUBA2	0.82	0.52	0.77
Actin-related protein 2/3 complex, subunit 1A (41 kDa)	AA490209	ARPC1A	0.73	0.46	0.36

Continued on facing page

TABLE 2—Continued

Function or protein description and gene name	Accession no.	Gene symbol	Change (fold) at time (h) postinfection		
			2.00	6.00	16.00
<b>Enzymes</b>					
6-Pyruvoyl-tetrahydropterin synthase/dimerization cofactor of hepatocyte nuclear factor 1 alpha	AA459909	PCBD	0.75	0.67	0.62
3-Hydroxyanthranilate 3,4-dioxygenase	AI005031	HAAO	0.90	0.89	0.6
COX11 (yeast) homolog, cytochrome <i>c</i> oxidase assembly protein	AA450001	COX11	0.71	0.61	0.61
Crystallin, beta B2	AA191518	CRYBB2	0.68	0.62	0.62
DNA segment, single-copy probe LNS-CAI/LNS-CAII (deleted in polyposis)	H99681	D5S346	0.67	0.62	0.64
Early growth response 2 (Krox-20 [ <i>Drosophila</i> ] homolog)	AA446027	EGR2	0.66	0.59	0.61
NADH dehydrogenase (ubiquinone) 1 alpha subcomplex, 2 (8 kDa, B8)	AI017426	NDUFA2	0.78	0.35	0.31
NADH dehydrogenase (ubiquinone) 1 alpha subcomplex, 9 (39 kDa)	AA598884	NDUFA9	0.65	0.66	0.59
Acetyl-coenzyme A acyltransferase 2 (mitochondrial 3-oxoacyl-coenzyme A thiolase)	H07926	ACAA2	0.73	0.59	0.56
<b>Immune response</b>					
CD39 antigen	H10011	CD39	0.54	0.58	0.85
CD59 antigen p18–20	H60549	CD59	0.85	0.52	0.44
CD6 antigen	AI336940	CD6	0.46	0.64	0.41
Coagulation factor V (proaccelerin, labile factor)	AA680136	F5	0.59	0.44	0.40
Interferon inducible	AA464417	IFITM3	0.58	0.55	0.24
Interleukin 1 receptor antagonist	T72877	IL1RN	0.55	0.49	0.46
Delta sleep-inducing peptide, immunoreactor	AA775091	DSIPI	0.65	0.5	0.26
<b>Ribosomal proteins</b>					
Ribosomal protein S29	N93715	RPS29	0.69	0.48	0.37
Ribosomal protein S4, X-linked	AA888182	RPS4X	0.69	0.48	0.37
Ribosomal protein L6	AA629808	RPL6	0.75	0.61	0.48
Ribosomal protein S16	AA668301	RPS16	0.76	0.60	0.54
<b>Degradation machinery</b>					
Ubiquitin carrier protein E2-C	AA430504	UBCH10	0.61	0.52	0.39
Ubiquitin-specific protease 5 (isopeptidase T)	AA465536	USP5	0.56	0.5	0.50
Ubiquitin-specific protease 5 (isopeptidase T)	AA465536	USP5	0.56	0.5	0.50
Ubiquitin-like 1 (sentrin)	AA488626	UBL1	0.68	0.58	0.5
<b>Transcription</b>					
General transcription factor IIIC, polypeptide 2 (beta subunit, 110 kDa)	AA922691	GTF3C2	0.78	0.57	0.52
Transcription factor 12 (HTF4, helix-loop-helix transcription factors 4)	H98856	TCF12	0.69	0.80	0.84
General transcription factor IIIC, polypeptide 2 (beta subunit, 110 kDa)	AA922691	GTF3C2	0.78	0.57	0.52
<b>Splicing</b>					
Splicing factor proline/glutamine rich (polypyrimidine tract binding protein associated)	AA425853	SFPQ	0.56	0.24	0.44
Splicing factor (CC1.3)	AA193573	CC1.3	0.65	0.62	0.23

<sup>a</sup> Genes in each cluster are grouped according to predicted biological function.

an internal control. The RT-PCR data confirmed the microarray results, showing the same relative transcription regulation of the selected genes (Table 3). These findings validate those of the Northern and microarray analyses. Absolute values are not identical when microarray and RT-PCR data are compared, probably due to intrinsic differences in the techniques.

**Target verification by Western blot analysis and ELISA of representative cell proteins.** To correlate transcription changes with protein levels, we defined the effects of MVA infection on some cellular components, analyzing protein expression levels by Western blotting. After MVA infection, microarray data indicated that tubulin expression was downregulated (Table 2),

a finding confirmed by Western blotting (Fig. 5A). Although actin gene expression was downregulated after 2 h postinfection in microarray analysis (Table 2), the protein was present in equal amounts in mock-infected and MVA-infected cells at 2, 6, and 16 h postinfection (Fig. 5A). This result is probably due to the stability of actin. Similar results were obtained with WR-infected HeLa cells (Fig. 5A). These findings show that the correlation between mRNA and protein levels depends on protein stability.

For other proteins, we confirmed microarray data with protein expression patterns. For these analyses, we used the Rho family small GTP-binding protein (RAC-1), the WASP family

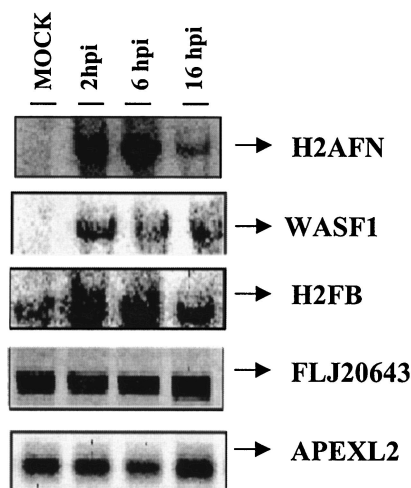


FIG. 4. Validation of microarray data by Northern blotting. Total RNA (20  $\mu$ g) purified from uninfected or MVA-infected cells at 2, 6, and 16 h postinfection was hybridized with probes derived from the PCR products spotted on the microarray. Genes included in the autoradiogram are H2AFN (histone N), WASF1 (Wiskott-Aldrich syndrome protein), H2FB (histone B), FLJ20643 (EST), and APEXL2 (apurinic/apuridinic endonuclease). hpi, hours postinfection.

member WAVE (WASF1), and the nuclear factor kappa light polypeptide (NFK $\beta$ 1). The RAC-1 protein signal increased in MVA-infected cells, with a peak at 6 h postinfection (Fig. 5B). At this time point, the amount of RAC-1 in MVA-infected cells was about threefold higher than that in control cells. WAVE showed a peak of expression at 16 h postinfection, when the amount of protein was about threefold higher than that in control cells. NF- $\kappa$ B protein expression was more than threefold higher than that in controls at 16 h postinfection, whereas there was no evidence of protein increases at early times postinfection (Fig. 5B). In the case of WR-infected cells, WAVE protein levels were similar for WR- and MVA-infected cells. RAC-1 and NF- $\kappa$ B showed different levels of protein expression at 16 h postinfection; these levels increased with MVA infection and decreased with WR infection (Fig. 5B). Evidence that viral late gene functions are necessary for the increases in RAC-1, WAVE, and NF- $\kappa$ B protein levels was

obtained (Fig. 5B) by Western blot analysis of MVA-infected cells cultured in the presence of cytosine-arabino- (AraC) and an inhibitor of viral DNA replication (21). Moreover, the increase in RAC-1, WAVE, and NF- $\kappa$ B protein expression required de novo protein synthesis, since the accumulation of these proteins was prevented by cycloheximide treatment (Fig. 5B). This result eliminates the possibility that MVA infection might increase protein levels by enhancing protein stability.

We further analyzed the levels of IL-6 and IFN- $\gamma$  secreted after MVA infection to confirm the data obtained by microarrays and quantitative RT-PCR. The amounts of secreted IL-6 and IFN- $\gamma$  were determined by ELISA with uninfected and MVA-infected HeLa cells (5 PFU/cell) at 2, 6, and 16 h postinfection. In agreement with data obtained in microarray and quantitative RT-PCR analyses, there was no detectable IFN- $\gamma$  in supernatants from MVA-infected cells (Fig. 5C). In contrast, we observed a strong increase with time in the amount of secreted IL-6 after MVA infection, in full agreement with the microarray and quantitative RT-PCR data (Fig. 5C). When HeLa cells were WR-infected, no IL-6 or IFN- $\gamma$  was detected by ELISA in cell-free supernatants (Fig. 5C).

## DISCUSSION

The interaction between viruses and the host cell are complex, multifaceted processes. While viruses attempt to take over cellular functions to their advantage, the cell counteracts by mounting a variety of defensive responses that may include induction of interferon, stress response, or apoptotic pathways, all of which are accompanied by changes in gene expression.

In this study, we analyzed the response of the human HeLa cell line to MVA infection by using cDNA microarrays. It was reported previously that MVA undergoes limited replication in HeLa cells (7, 11, 14); virus replication is restricted during infection of HeLa cells after immature virions are formed (7, 14, 34, 36), allowing efficient production of proteins (33, 37, 42). Due to the interest in MVA-based vectors as potential vaccines against pathogens and tumors and current phase I clinical trials with this vector, there is a need to understand the host response to MVA infection. We used microarrays to analyze the changes in host gene expression profiling after MVA infection of cultured human cells.

A total of 410 of 13,295 genes in the array were significantly regulated after MVA infection and assigned to 11 clusters (Fig. 2). Clusters 1 and 2 included 68 genes that were upregulated at 2, 6, and 16 h postinfection. A total of 58 genes were identified in cluster 3; their expression increased at 2 and 6 h postinfection. In cluster 4, we observed 15 genes upregulated at 6 and 16 h postinfection. In cluster 5, 11 genes were downregulated at 2 h but upregulated at 6 and 16 h postinfection. The 11 genes in cluster 6 were upregulated only at 2 h postinfection. The remaining genes, a total of 247, were downregulated with different expression profiling and are represented in clusters 6 to 11 (Table 2). Indeed, these findings differ from the host transcriptional responses observed after WR infection, for which only 37 cellular genes were upregulated in HeLa cells infected at 2, 6, and 16 h postinfection (17). A comparison of gene expression profiles based on data obtained in this study and those from previous work with WR (17) is shown for representative genes in Table 4. In MVA- or WR-infected HeLa

TABLE 3. Confirmation of microarray data by quantitative real-time RT-PCR<sup>a</sup>

Gene product	Change (fold) determined by assay at time (h) postinfection					
	Microarray			RT-PCR		
	2	6	16	2	6	16
H2BFB	9.92	10.20	17.03	25	18	19
PCNT2	3.94	3.14	2.17	4.36	4.44	3.4
WASF1	3.01	2.66	1.11	3.73	2.72	1.53
WAS	2.58	2.25	1.61	5.08	15.2	2.3
IL7	6.10	5.30	3.2	6.86	5.8	4.9
IL6	2.45	3.02	1.90	1.75	2.07	2.28
IFNG	1.27	1.36	1.45	1.35	1.15	1.19
APEXL2	1.10	0.98	1.11	0.96	1.2	0.84
FLJ	0.98	1.25	1.01	1.1	1.02	0.93

<sup>a</sup> RT-PCR conditions are described in Materials and Methods.

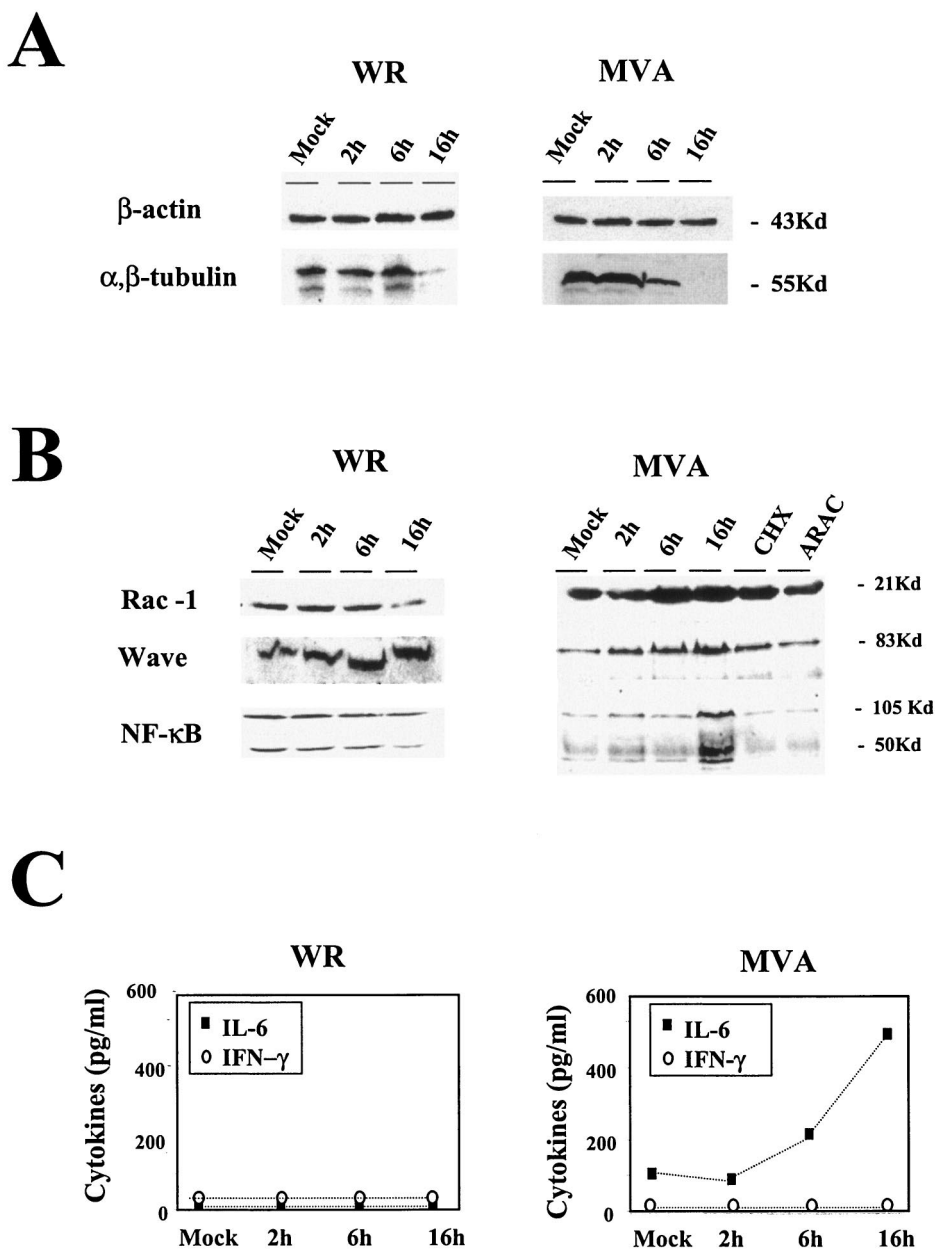


FIG. 5. Validation of microarray data by protein level and comparison between MVA and WR infections. Shown are Western blots of different cellular proteins at various times (2, 6, and 16 h postinfection). (A) Actin and tubulin protein levels in HeLa cells (5 PFU/cell). (B) RAC-1, WAVE, and NF- $\kappa$ B protein levels in MVA- or WR-infected HeLa cells (5 PFU/cell) and in cells infected with MVA in the presence of cycloheximide (CHX; 100  $\mu$ g/ml) or cytosine arabinoside (ARAC; 50  $\mu$ g/ml) for 16 h. (C) Levels of IL-6 and IFN- $\gamma$  secreted from HeLa cells after MVA or WR infection (5 PFU/cell), as determined by ELISA. Protein levels of IL-6 and IFN- $\gamma$  in supernatants of uninfected and MVA- or WR-infected cells were measured at 2, 6, and 16 h postinfection. Duplicate samples were measured in two independent experiments. Kd, kilodaltons

cells, there is a group of cellular genes upregulated by both viruses; other genes are upregulated selectively by MVA or WR, and a large number of genes are downregulated by both viruses. These results suggest that MVA and WR use different strategies to regulate cellular transcriptional responses, probably as a consequence of deletions in the MVA genome. This idea is supported by the observed differences in MVA-induced CPE and shutoff of host protein synthesis and those induced by WR (Fig. 1) and is consistent with previous results of analyses of the biology of MVA (14, 33).

Examination and analysis of the list of the cellular genes upregulated by MVA indicated several gene families with significant, distinct biological functions (Table 1). Some of these groups include genes involved in adhesion, the cytoskeleton, the cell cycle, apoptosis, histone, and immune modulation. Some of these genes may be involved in processes such as viral replication or cell defense.

Transcription of several genes involved in the immune response (20 transcripts) was activated by MVA infection. At least five cytokines (IL-1A, IL-6, IL-7, IL-8, and IL-15) and five

TABLE 4. Representative gene expression profiling of WR and MVA strains in human HeLa cells<sup>a</sup>

Effect and gene name	Gene symbol	Change (fold) with strain at time (h) postinfection					
		MVA			WR		
		2	6	16	2	6	16
<b>Increased genes in MVA and WR</b>							
Pericentrin	PCNT	3.94	3.14	2.38	3.20	7.11	1.58
Claudin 3	CLDN3	2.54	2.48	1.32	1.78	2.13	2.30
H3 histone family, member B	H3FB	16.34	15.67	21.71	4.92	1.12	1.11
CD80 antigen	CD80	4.29	3.36	2.57	1.75	2.58	2.06
Thymosin beta 4 X chromosome	TMSB4X	3.81	5.7	2.91	3.81	5.70	2.91
Adenosine A2a receptor,	ADORA2A	3.89	4.14	4.11	3.89	4.14	4.11
WAS protein family, member 1	WASF1	3.01	2.66	2.11	2.35	2.43	2.99
H3 histone family, member B	H3FB	16.34	15.67	21.71	1.17	1.12	1.11
H4 histone family, member D	H4FD	12.38	24.93	24.93	2.41	0.97	1.01
H2B histone family, member B	H2BFB	9.92	10.20	17.03	5.94	0.78	0.61
<b>Increased genes in MVA</b>							
Interleukin 7	IL-7	6.1	5.3	3.2	1.12	0.95	0.76
B7 protein	B7	1.97	1.75	3.53	1.03	0.94	0.88
CD47 antigen	CD47	5.35	4.08	3.16	1.1	0.99	1.01
Interleukin 6	IL-6	2.65	2.14	1.56	1.32	0.87	1.06
Nuclear factor of kappa light polypeptide epsilon	NFKBIE	2.41	1.61	1.12	1.01	1.01	0.75
Mitogen-activated protein kinase kinase 5	MAP2K5	2.37	2.74	1.69	1.06	1.23	0.69
Nuclear factor (erythroid-derived 2)-like 3	NFE2L3	2.36	2.36	2.52	1.12	0.89	1.01
Nuclear factor of kappa light polypeptide 2	NFKB2	2.03	2.22	2.34	1.2	0.54	0.59
Kinesin family member 5A	KIF5A	2.05	1.88	1.73	2.31	0.17	0.17
Nuclear factor of activated T cells, cytoplasmic 3	NFATC3	3.46	2.97	1.30	1.01	0.97	1.33
<b>Increased genes in WR</b>							
Diacylglycerol kinase delta	DGKD	1.32	1.56	1.59	2.01	1.17	0.9
Selenophosphate synthetase	SPS	1.12	1.32	0.95	3.73	7.11	2.17
Glutamate decarboxylase 2 (pancreatic islets and brain, 65 kDa)	GAD2	1.98	1.1	0.74	3.56	2.38	3.14
Golgi resident protein	GCP60	1.02	0.87	0.65	1.41	2.00	1.79
<b>Decreased genes in MVA and WR</b>							
ATP synthase, subunit c (subunit 9), isoform 2	ATP9C2	0.84	0.21	0.16	1.43	0.20	0.09
ATP synthase, subunit b, isoform 1	ATP1B	0.53	0.40	1.12	1.39	0.18	0.12
Cytochrome c-1	CYC1	0.71	0.37	0.23	0.30	0.21	0.04
Tubulin, beta 2	TUBB2	0.84	0.79	0.48	0.73	0.22	0.26
Actin, alpha 2, smooth muscle, aorta	ACTA2	0.76	0.47	0.44	0.84	0.56	0.12
Interleukin 1 receptor antagonist	IL1RN	0.55	0.49	0.46	0.15	0.21	0.18
Macrophage stimulating 1 (hepatocyte growth factor-like)	MST1	0.68	0.65	0.74	0.55	0.16	0.11
Ribosomal protein S27a	RPS27A	0.85	0.58	0.72	0.84	0.34	0.43
Ribosomal protein S28	RPS28	0.89	0.63	0.69	0.65	0.31	0.41
Ubiquitin carrier protein E2-C	UBCH10	0.61	0.52	0.39	0.78	0.24	0.26
Proteasome (prosome, macropain) subunit, beta type 3	PSMB3	0.98	0.69	0.71	0.50	0.17	0.17

<sup>a</sup> Representative groups of genes from the microarray data obtained for MVA (this report) and from previous work with WR (17) were selected according to their up- or downregulation. For comparative purposes, we show cellular genes that are upregulated by both viruses, genes that are upregulated selectively by MVA or WR, and genes that are downregulated by the two viruses. Genes in each cluster were grouped according to predicted biological function.

members of the tumor necrosis factor receptor (TNF) family (TNFRSF7, TNFAIP3, TNFRSF14, TNFRSF17, and TRAF3) were upregulated in response to MVA. Genes encoding CD47 and CD80 antigens showed marked inductions at early and late times after MVA infection (Table 1). The immune modulator gene IL-7 upregulation was more than sixfold compared to levels for control cells at early times postinfection (Table 1), a result validated by quantitative RT-PCR (Table 3). The MVA-induced increase in IL-15 gene expression is a characteristic also observed for other viruses (3). At the protein level, we observed elevated IL-6 levels in supernatants from MVA-infected HeLa cells but not in those from cells infected with WR (Fig. 5C). A similar increase in IL-6 and TNF- $\alpha$  levels was found in spleen homogenates from MVA-infected mice but not in those from WR-infected mice (33). These results indi-

cate that MVA and WR induce different proinflammatory cytokine profiles both in vivo and in vitro.

We observed clear upregulation of NF- $\kappa$ B expression during MVA infection, as determined by mRNA (Table 1) and protein levels (Fig. 5B). In the case of WR, NF- $\kappa$ B expression was downregulated at late times postinfection (Table 4). The increase in NF- $\kappa$ B protein required viral DNA replication, as seen with cells infected in the presence of adenosine arabinoside, an inhibitor of virus DNA synthesis. Moreover, the increase in NF- $\kappa$ B protein levels required de novo protein synthesis, as observed after cycloheximide treatment (Fig. 5B). These findings concur with the observation by Oie and Pickup (31) of an increase in NF- $\kappa$ B activity in extracts from MVA-infected 293 cells but not in cells infected with the Copenhagen strain of VV. The NF- $\kappa$ B family has a central role in the

transcriptional regulation of inflammatory cytokines and other genes essential for activating immune responses (10). NF- $\kappa$ B also regulates the expression of genes involved in the control of cell proliferation and apoptosis (10, 31). It can be speculated that the increase observed in NF- $\kappa$ B mRNA and protein levels in response to MVA infection corresponds to enhanced NF- $\kappa$ B activity. An increase in NF- $\kappa$ B protein levels, together with the I $\kappa$ B- $\alpha$  degradation previously observed in MVA-infected cells (31), will contribute to the transcription of  $\kappa$ B-dependent genes and to the clearance of virus infection as a result of the induction of apoptosis and specific immune responses. Since MVA has large genome deletions, viral genes that interfere with NF- $\kappa$ B, present in orthopoxviruses, might be absent (31).

In accord with previous microarray results for WR-infected cells (17), we observed increased levels of WASF1, claudin 3, CD-80, thymosin-beta-4, and adenosine-A2a receptor during MVA infection (Table 4). Comparison of WR and MVA nonetheless showed differences in expression levels of other genes, including kinesin-5 and histone family members, during infection. In WR-infected cells, these genes were upregulated early but not late in infection, whereas in MVA-infected cells, levels were maintained throughout infection. Among genes with an important role in motility and WR spreading is the Wiskott-Aldrich syndrome protein family member N-WASP (WASL gene) (13). WAS and WASF1 were upregulated in MVA-infected cells, whereas in WR-infected cells, only WASF1 was upregulated. Significantly, the small GTP-binding protein RAC-1 was also induced after MVA infection. Although the role of WAS proteins in the cell is well established (6, 27), the biological meaning of WASP family upregulation by a nonproductive virus is not immediately clear, in contrast to the case for WR, in which it appears to be important for viral spreading (6, 26, 38, 39).

It was reported that MVA has lost functional receptors for TNF, IFN- $\gamma$ , IFN $\alpha/\beta$ , and CC chemokines (4, 7, 28, 29). The absence of these viral proteins and the induction of different host immune response molecules such as TNF may be the reason for MVA attenuation and for the potent immune response elicited by MVA recombinants to specific antigens compared with that elicited by VV recombinants (33). Induction of innate and adaptive immune responses during MVA infection could have a beneficial effect when MVA is used as a vaccine. MVA is known to trigger a poor immune response against itself, while it activates a potent immune response to specific antigens delivered by the vector (33). The enhanced expression of genes encoding immunomodulatory molecules (Table 1) during MVA infection might create a microenvironment that allows antigen-presenting cells and activated T cells to help expand CD4<sup>+</sup> and CD8<sup>+</sup> T cell populations. This possibility may be relevant when immunization protocols that include prime-booster immunization with heterologous vectors are used (33, 35). Maintenance of specific T cells could contribute to MVA-induced expression of cytokines such as IL-15. MVA induction of cellular genes with immunomodulatory functions may be a major contributing factor in the enhanced immunogenicity of MVA-derived vaccines.

In conclusion, through analyses of host cell gene expression profiling after MVA infection of cultured human cells, we found a number of cellular genes whose expression levels are markedly modified by MVA infection and suggest potential

roles as regulators of viral infection. Some of these upregulated genes may be involved in the enhanced immune response to specific antigens observed in animals after infection with MVA recombinants. Identification of genes that are differentially regulated and the characterization of their functions is important when the potential benefit of MVA as a vector for vaccination against pathogens and tumors is considered.

#### ACKNOWLEDGMENTS

We are indebted to R. Bablanian, M. Krupa, and C. Mark for critical reviews of the manuscript, to J. C. Gallego for kindly providing the RAC-1 antibody, to J. C. Oliveros for bioinformatic assistance, and to V. Jiménez for expert technical assistance.

This work was supported by grants from the Spanish Ministry of Science and Technology (grants BIO2000-0340P4 and BIO2001-2269), the Spanish Foundation for AIDS Research (grant FIPSE 36344/02), and the EU (grants QLRT-PL-1999-01321 and QLK2-CT-2002-01867) to M.E. A.P.-M was partially supported by Spanish CICYT grant number BIO2001-1237. The Department of Immunology and Oncology was founded and is supported by the Spanish Council for Scientific Research (CSIC) and Pfizer.

#### REFERENCES

1. Altenburger, W., C.-P. Sütter, and J. Altenburger. 1989. Partial deletion of the human host range in the attenuated vaccinia virus MVA. *Arch. Virol.* **105**:15–27.
2. Antonie, G., F. Scheiflinger, F. Dorner, and F. G. Falkner. 1998. The complete genomic sequence of the modified vaccinia Ankara strain: comparison with other orthopoxviruses. *Virology* **244**:365–396.
3. Azimi, N., K. Brown, R. N. Bamford, Y. Tagaya, U. Siebenlist, and T. A. Waldmann. 1998. Human T cell lymphotropic virus type I Tax protein trans-activates interleukin 15 gene transcription through an NF- $\kappa$ B site. *Proc. Natl. Acad. Sci. USA* **95**:2452–2457.
4. Blanchard, T. J., A. Alcami, P. Andrea, and G. L. Smith. 1998. Modified vaccinia virus Ankara undergoes limited replication in human cells and lacks several immunomodulatory proteins: implication for use as a human vaccine. *J. Gen. Virol.* **79**:1159–1167.
5. Bolt, G., K. Berg, and M. Blixenkrone-Møller. 2002. Measles virus-induced modulation of host-cell gene expression. *J. Gen. Virol.* **83**:1157–1165.
6. Caron, E. 2002. Regulation of Wiskott-Aldrich syndrome protein and related molecules. *Curr. Opin. Cell Biol.* **14**:82–87.
7. Carroll, M. W., and B. Moss. 1997. Host range and cytopathogenicity of the highly attenuated MVA strain of vaccinia virus: propagation and generation of recombinant viruses in a nonhuman mammalian cell line. *Virology* **238**:198–211.
8. Carroll, M. W., W. W. Overwijk, R. S. Chamberlain, S. A. Rosenberg, B. Moss, and N. P. Restifo. 1997. Highly attenuated modified vaccinia virus Ankara (MVA) as an effective recombinant vector: a murine tumor model. *Vaccine* **15**:387–394.
9. Chang, Y. E., and L. A. Laimins. 2000. Microarray analysis identifies interferon-inducible genes and stat-1 as major transcriptional target of human papillomavirus type 31. *J. Virol.* **74**:4174–4182.
10. Chen, F., V. Castranova, X. Shi, and L. M. Demers. 1999. New insights into the role of nuclear factor- $\kappa$ B, a ubiquitous transcription factor in the initiation of diseases. *Clin. Chem.* **45**:7–17.
11. Drexler, I., K. Heller, B. Wahren, V. Erfle, and G. Sütter. 1998. Highly attenuated modified vaccinia virus Ankara replicates in baby hamster kidney cells, a potential host for virus propagation, but not in various human transformed and primary cells. *J. Gen. Virol.* **79**:347–352.
12. Eisen, M. B., P. T. Spellman, P. O. Brown, and D. Botstein. 1998. Cluster analysis and display of genome-wide expression patterns. *Proc. Natl. Acad. Sci. USA* **95**:14863–14868.
13. Frischknecht, F., V. Moreau, S. Rottger, I. Reckmann, C. Superti-Furga, and M. Way. 1999. Actin based motility of vaccinia virus mimics receptor tyrosine kinase signalling. *Nature* **404**:1007–1011.
14. Gallego-Gómez, J. C., C. Risco, D. Rodriguez, P. Cabezas, S. Guerra, J. L. Carrascosa, and M. Esteban. 2003. Differences in virus-induced cell morphology and virus maturation between the WR and MVA strains of vaccinia virus. *J. Virol.* **77**:10606–10622.
15. García de la Nava, J., D. Franco Santaella, J. Cuenca Alba, J. M. Carazo, O. Trelles, and A. Pascual-Montano. 2003. Engene: the processing and exploratory analysis of gene expression data. *Bioinformatics* **19**:657–658.
16. Geiss, G. K., R. E. Bumgarner, M. C. An, A. B. Agy, A. B. van't Wout, E. Hammersmark, V. S. Carter, D. Upchurch, J. I. Mullins, and M. G. Katze. 2001. Large-scale monitoring of host gene expression during HIV-1 infection using cDNA microarrays. *Virology* **266**:8–16.

17. Guerra, S., L. A. López-Fernandez, A. Pascual-Montano, M. Muñoz, K. Harshman, and M. Esteban. 2003. Cellular gene expression survey of vaccinia virus infection of human HeLa cells. *J. Virol.* **77**:6493–6506.
18. Hirsch, V. M., T. R. Fuerst, G. Sutter, M. W. Carroll, L. C. Yang, S. Goldstein, M. Piatak, Jr., W. R. Elkins, W. G. Alvord, D. C. Montefiori, B. Moss, and J. D. Lifston. 1996. Patterns of viral replication correlate with outcome in simian immunodeficiency virus (SIV)-infected macaques: effect of prior immunization with a trivalent SIV vaccine in modified vaccinia virus Ankara. *J. Virol.* **70**:3741–3752.
19. Hughes, T. R., M. J. Marton, A. R. Jones, C. J. Roberts, R. Stoughton, C. D. Armour, H. A. Bennett, E. Coffey, H. Dai, Y. D. He, M. J. Kidd, A. M. King, M. R. Meyer, D. Slade, P. Y. Lum, S. B. Stepaniants, D. D. Shoemaker, D. Gachotte, K. Chakraburttty, J. Simon, M. Bard, and S. H. Friend. 2000. Functional discovery via a compendium of expression profiles. *Cell* **102**:109–126.
20. Jones, J. O., and A. M. Arvin. 2003. Microarray analysis of host cell gene transcription in response to Varicella-Zoster virus infection of human T cells and fibroblasts in vitro and SCIDhu skin xenografts in vivo. *J. Virol.* **77**:1268–1280.
21. Keck, J. G., C. J. Baldick, Jr., and B. Moss. 1990. Role of DNA replication in vaccinia virus gene expression: a naked template is required for transcription of three late trans-activator genes. *Cell* **61**:801–809.
22. Kohonen, T. 1997. Self-organizing maps, 2nd ed. Springer-Verlag, Heidelberg, Germany.
23. Mahnel, H., and A. Mayr. 2002. Experiences with immunization against orthopox viruses of humans and animals using vaccine strain MVA. *Berl. Muench. Tieraerztl. Wochenschr.* **107**:253–256.
24. Mayr, A., H. Stickl, H. K. Muller, K. Danner, and H. Singer. 1978. The smallpox vaccination strain MVA: marker, genetic structure, experience gained with parenteral vaccination and behaviour in organism with a debilitated defense mechanism. *Zentbl. Bakteriol. B* **167**:375–390.
25. Meyer, H., G. Sutter, and A. Mayr. 1991. Mapping of deletions in the genome of highly attenuated vaccinia virus MVA and their influence on virulence. *J. Gen. Virol.* **72**:1031–1038.
26. Miki, H., K. Minura, and T. Takenawa. 1996. N-WASP, a novel actin-depolymerizing protein, regulates the cortical cytoskeletal rearrangement in a PIP2-dependent manner downstream of tyrosine kinases. *EMBO J.* **15**:5326–5335.
27. Moreau, V., F. Frischknecht, I. Reckmann, G. Superti-Furga, and M. Way. 2000. A complex of N-WASP and WIP integrates signalling cascades that lead to actin polymerization. *Nat. Cell Biol.* **2**:441–448.
28. Moss, B., M. W. Carroll, L. S. Wyatt, J. R. Bennink, V. M. Hirsch, S. Goldstein, W. R. Elkins, W. Overwijk, R. Chamberlain, S. A. Rosenberg, and G. Sutter. 1996. Host range restricted, non-replicating vaccinia virus vectors as vaccine candidates. *Adv. Exp. Med. Biol.* **397**:7–13.
29. Moss, B., and J. L. Shisler. 2001. Immunology 101 at poxvirus U: immune evasion genes. *Semin. Immunol.* **13**:59–66.
30. Nees, N., J. M. Geoghegan, T. Hyman, S. Frank, L. Miller, and C. D. Woodworth. 2001. Papillomavirus type 16 oncogenes downregulate expression interferon-responsive genes and upregulate proliferation-associated and NF- $\kappa$ B-responsive genes in cervical keratinocytes. *J. Virol.* **75**:4283–4296.
31. Oie, L. K., and D. Pickup. 2001. Cowpox and other members of the orthopoxvirus genus interfere with the regulation of NF- $\kappa$ B activation. *Virology* **288**:175–187.
32. Quackenbush, J. 2002. Microarray data normalization and transformation. *Nat. Genet.* **32**:496–501.
33. Ramirez, J. C., M. M. Gherardi, and M. Esteban. 2000. Biology of attenuated modified vaccinia virus Ankara recombinant vector in mice: virus fate and activation of B- and T-cell immune responses in comparison with the Western Reserve strain and advantages as a vaccine. *J. Virol.* **74**:923–933.
34. Sancho, M. C., S. Schleich, G. Griffiths, and J. Krijnse-Locker. 2002. The block in assembly of modified vaccinia virus Ankara in HeLa cells reveals new insights into vaccinia virus morphogenesis. *J. Virol.* **76**:8318–8334.
35. Schneider, J., S. C. Gilbert, T. J. Blanchard, T. Hanke, K. J. Robson, C. M. Hannan, M. Becker, R. Sinden, G. L. Smith, and A. V. S. Hill. 1998. Enhanced immunogenicity for CD8+ T cell induction and complete protective efficacy of malaria DNA vaccination by boosting with modified vaccinia virus Ankara. *Nat. Med.* **4**:397–402.
36. Sütter, G., and B. Moss. 1992. Nonreplicating vaccinia vector efficiently expresses recombinant genes. *Proc. Natl. Acad. Sci. USA* **89**:10847–10851.
37. Sütter, G., L. S. Wyatt, P. L. Foley, J. R. Bennink, and B. Moss. 1994. A recombinant vector derived from the host range-restricted and highly attenuated MVA strain of vaccinia virus stimulates protective immunity in mice to influenza virus. *Vaccine* **12**:1032–1040.
38. Symons, M., J. M. Derry, B. Karlak, S. Jiang, V. Lemahieu, F. McCormick, U. Francke, and A. Abo. 1996. Wiskott-Aldrich syndrome protein, a novel effector for the GTPase Cdc42Hs, is implicated in actin polymerization. *Cell* **84**:723–734.
39. Takenawa, T., and H. Miki. 2001. WASP and WAVE family proteins: key molecules for rapid rearrangement of cortical actin filaments and cell movement. *J. Cell Sci.* **114**:1801–1809.
40. Tamayo, P., D. Slonim, J. Mesirov, Q. Zhu, E. Dmitrovsky, E. S. Lander, and T. R. Golub. 1999. Interpreting patterns of gene expression with self-organizing maps: methods and application to hematopoietic differentiation. *Proc. Natl. Acad. Sci. USA* **96**:2907–2912.
41. van 't Wout, A. B., G. K. Lehrman, S. A. Mikheeva, G. C. O'Keeffe, M. G. Katze, R. E. Bumgarner, G. K. Geiss, and J. I. Mullins. 2003. Cellular gene expression upon human immunodeficiency virus type 1 infection of CD4+ T-cell lines. *J. Virol.* **77**:1392–1402.
42. Wyatt, L. S., M. W. Carroll, C.-P. Czerny, M. Merchlinsky, J. R. Sisler, and B. Moss. 1998. Marker rescue of the host range restrictions defects of modified vaccinia virus Ankara. *Virology* **251**:334–342.
43. Zhu, H., J. P. Cong, G. Mantora, T. Gineras, and T. Shenk. 1998. Cellular gene expression altered by human cytomegalovirus: global monitoring with oligonucleotide arrays. *Proc. Natl. Acad. Sci. USA* **95**:14470–14475.